THE ASTROPHYSICAL JOURNAL, 302:477–487, 1986 March 1

CO^+ FLUORESCENCE IN COMETS

LORIS MAGNANI AND MICHAEL F. A'HEARN
Astronomy Program, University of Maryland, College Park
Received 1985 April 11; accepted 1985 September 4

ABSTRACT

Calculations of the fluorescent equilibrium of the CO^+ molecule to determine the Swings and Greenstein effects as a function of heliocentric radial velocity have been carried out. The previously ignored Baldet-Johnson (*B–A*) bands were included in addition to the comet tail (*A–X*) and first negative (*B–X*) bands, thus allowing a determination of the absolute intensities of all bands. As with certain other molecules such as OH and CN, the Swings effect on individual lines is large enough that integrated band fluxes in the comet tail system also exhibit the Swings effect. The flux variations for velocities in the range -50 to $+350$ km s^{-1} have been calculated and may be used to map the acceleration of CO^+ ions into the tail, even with low-dispersion spectra.

Subject headings: atomic processes — comets

I. INTRODUCTION

In the tail of a comet, the major light-emitting ions are usually CO^+ and H_2O^+, with the H_2O^+/CO^+ ratio varying from comet to comet (Miller 1980). Because both ions exhibit band systems whose emission is primarily due to permitted electronic transitions in the visible region, resonance fluorescence via solar radiation should be the dominant exciting process. Calculations by Arpigny (1964*b*), Wyckoff and Wehinger (1976), and Krishna Swamy (1979) have demonstrated that this hypothesis, to the extent of their calculations, is consistent with the existing observations. Only Arpigny, however, has considered the rotational structure of the bands in the calculations; the others have considered only the electronic and vibrational structure and have therefore completely omitted the variations due to Doppler displacements of the exciting transitions. This phenomenon is known as the Swings effect (Swings 1941) when it is produced by the motion of the whole comet, and the Greenstein effect (Greenstein 1958) when it is due to material motion within the comet itself. These motions could cause variations in individual rotational line intensities or in overall band intensities which might be noticeable on existing spectroscopic plates or after future observations. Delsemme (1982) has mentioned this technique as a way of determining the expansion velocity of CN in the coma. This method, applied to CO^+, could lead to a positive resolution of the question of whether motions in cometary tails are due to bulk motion or to wave phenomena. This question is still an unresolved issue (see Brandt and Mendis 1979), and will be addressed in a separate paper.

II. MOLECULAR STRUCTURE OF CO^+

The overall structure of the *X*, *A*, and *B* states of the CO^+ molecule is shown in Figure 1. The model for the energy levels of the CO^+ molecule must include at least as many vibrational and rotational states as are necessary to reproduce the observed spectra. As an initial guess it is assumed that the presence of discernible lines in the cometary spectra of CO^+ and the strength of the Frank-Condon factor for a particular band indicate which vibrational and rotational levels are populated sufficiently to be significant in the calculation. Once the relative populations have been calculated, the populations of the highest rotational and vibrational levels can be checked to see that their populations are negligible compared to those of lower levels.

Emission has been observed from the (6, 0) and (6, 1) bands of the comet tail system (Swings and Page 1950; Arpigny 1964*b*). Hence, seven vibrational levels are included for the first excited electronic state, $A\ ^2\Pi$. The first negative band system (*B–X*) has been observed in comet West 1976 VI at moderate resolution with rocket instrumentation by Feldman and Brune (1976). The bands observed include: (1, 0), (2, 1), (0, 0), (1, 1), (1, 2), (0, 1), (1, 3), and (2, 4). This result, coupled with the vibrational transition probabilities (Frank-Condon factors of Jarmain, Fraser, and Nicholls 1955), implies that the $B\ ^2\Sigma^+$ state has significant population only for the lower vibrational states. Preliminary calculations showed that the population in the ground state was confined mostly to the $v = 0$ vibrational level. Nearly all the pumping arises from this level, so that only a few vibrational levels are needed within the ground electronic state in order to model correctly the strong bands of CO^+. The model therefore includes three vibrational levels for both Σ^+ states. It does not include the $v = 3$ or $v = 4$ levels of the $X\ ^2\Sigma^+$ state despite the presence of observed (1, 3) and (2, 4) *B–X* transitions. Those transitions are blended with the (0–2) band, and so it is unclear how much they contribute to the detected emission. Furthermore, preliminary calculations (with fewer rotational levels) indicated that the populations of these levels were small.

Arpigny (1964*b*) determined from a high-resolution spectrogram of comet Humason 1962 VIII that the rotational lines of a given branch of the blue ($A\ ^2\Pi_{1/2}$) 3–0 band of the comet tail system are visible out to at least $N = 6$ or 7. (N is the quantum number for molecular rotation, formerly known as K, and J is the quantum number for total angular momentum.) The plate was underexposed, leading Arpigny to speculate that the rotational lines would extend out to $N = 10$. High-resolution plates of comet Bennet 1970 II show rotational structure out to $N = 12$ (Arpigny, private communication). All rotational levels with $N \leq 10$ are included, a compromise dictated by computational limits. The calculations show that the population at $N = 10$ is down by almost an order of magni-

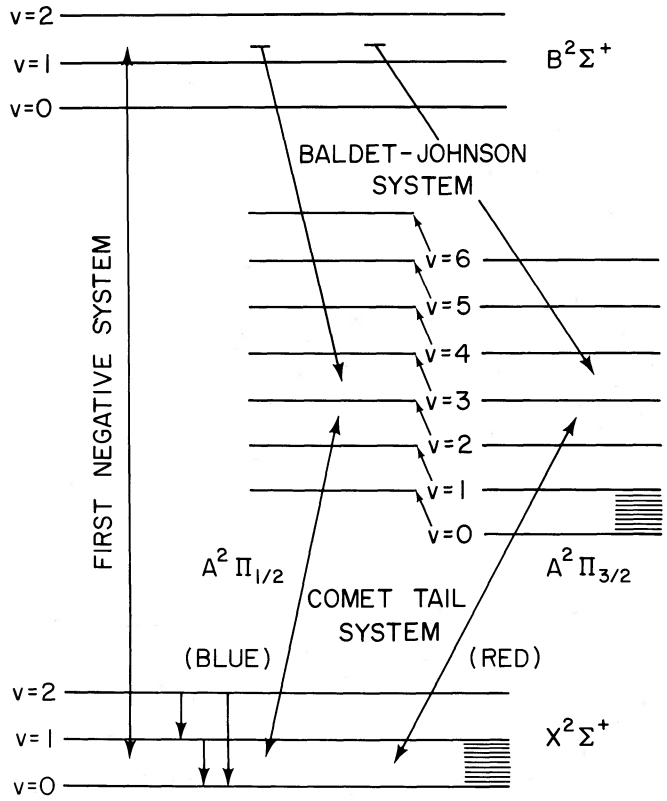

FIG. 1.—Energy level diagram for the $B\ ^2\Sigma^+$, $A\ ^2\Pi_i$, and $X\ ^2\Sigma^+$ electronic states of CO^+ (not drawn to scale). Calculations include electronic pumping in the first negative and comet tail systems and vibrational pumping within the $X\ ^2\Sigma^+$ state. Radiative decay is included for all electronic systems and for vibrorotational transitions within the $X\ ^2\Sigma^+$ state.

tude and clearly decreasing compared to the peak population, so that transitions from higher rotational levels will not contribute much to the luminosity of a band.

The rotational levels of the $X\ ^2\Sigma^+$ and $B\ ^2\Sigma^+$ states are split as a result of the interaction of the molecular rotation and electron spin ($\Sigma = \pm\frac{1}{2}$), with the resulting total angular momentum, $J = N \pm \frac{1}{2}$. Each rotational level in either of the $^2\Sigma^+$ states is therefore two separate levels, excepting the lowest level ($N = 0, J = \frac{1}{2}$), which has only one component. This splitting in the $^2\Sigma^+$ states is negligible (of order 0.10 cm^{-1}), because the $^2\Sigma^+$ coupling belongs to Hund's case b (for details see Herzberg 1950). Each doubled rotational level is treated as one level in the final calculation to minimize the number of simultaneous equations. However, for the calculations of the Hönl-London factors, for Einstein A- and B-coefficients, and for general bookkeeping purposes, the doubled levels are treated as two separate levels which are combined and renormalized to yield the final coefficients for the system of linear equations (see § III).

The $A\ ^2\Pi$ state is divided into two branches ($^2\Pi_{1/2}$ and $^2\Pi_{3/2}$) by the same effect, but with a much larger separation because the $^2\Pi$ electronic state is intermediate between Hund's cases a and b. In addition, each set of energy levels ($A\ ^2\Pi_{1/2}$ and $A\ ^2\Pi_{3/2}$) has its rotational levels split as a result of Λ-doubling, the phenomenon in which the interaction of the angular momentum of molecular rotation with the electronic orbital angular momentum removes the degeneracy of the two components of a Π-term. Each rotational level split by Λ-doubling is in turn subject to hypefine splitting. Hyperfine transitions are not included in our model, and, in the same way as outlined above, the Λ-doubled components of the $^2\Pi_{1/2}$ and $^2\Pi_{3/2}$ branches are treated as separate levels until the final step where the population of the levels is calculated. The inclusion of all the transitions mentioned leads to a model for the CO^+ molecule consisting of 206 separate levels.

The selection rules involved in electrostatic dipole transitions for diatomic molecules are (1) the parity must change, and (2) $\Delta J = 0, \pm 1$. The resulting branches have been designated in various ways. Using current conventions for spectroscopic notation, the branches of a band are named P, Q, or R according to the value of $\Delta J = J' - J'' = -1, 0$, or $+1$. The value of $\Delta N = N' - N''$ $(-2, -1, 0, +1, +2)$ is given by a left superscript of O, P, Q, R, or S. A subscript "1" indicates that $N = J - \frac{1}{2}$, and a subscript "2" indicates that $N = J + \frac{1}{2}$. If the subscript is the same for both upper and lower states, the subscript is given only once; if the subscript is different, then the upper value is given first. The value of J'' is given in parentheses after the branch and term notations. This notation differs from that of Rao (1950*a*, *b*). Hence, ${}^rQ_{12}(7/2)$ represents a transition from the level with $N' = 3$, $J' = 7/2$ to the level with $N'' = 4$, $J'' = 7/2$ and opposite parity.

III. CALCULATIONS

a) Theory

The population of the energy levels of CO^+ molecules in equilibrium with the radiation field may be determined by equating the sum of the transition probabilities out of each level with the sum of the transition probabilities into that level. The Einstein A- and B-coefficients (with B multiplied by the energy density of the radiation field) express the transition probabilities between two levels, and thus they are the coefficients of the resulting simultaneous linear equations. For electronic transitions, the excitations by any process other than reasonance fluorescence have been neglected since the time scales for other processes are too long to affect the population (Arpigny 1976). The particle density beyond 10^4 km is too low to allow collisions to populate even the lowest rotational levels of most of the observed radicals and ions (Crovisier 1985). In addition, the pumping rate out of the lowest rational levels is much greater than the collisional excitation rate. Consequently, collisional transitions have been ignored in the calculations.

The total absorption rate of solar photons at 1 AU out of given rotational levels in the $v = 0$ state of the ground electronic state occurs on time scales of order 1 s. Given 10 rotational levels in the $v = 0$ state, it would take on the order of 10 cycles to populate all these rotational levels via fluorescence. The time scale for the fluorescence to cycle through all the levels of the ground state is therefore of order tens of seconds, which is substantially less than the lifetime of CO^+. This ensures that by the time CO^+ is detected in the tail of a comet, the great majority of molecules are in fluorescent equilibrium.

The process described above may be written for level j:

$$\sum_{i=j+1}^{n} (A_{ij}\, x_i - B_{ji}\, \rho_{\nu_{ij}}\, x_j) - \sum_{i=1}^{j-1} (A_{ji}\, x_j - B_{ij}\, \rho_{\nu_{ij}}\, x_i) = 0\ ,$$

where n is the number of levels, x is the fractional population of the level j or i, and ρ is the radiation energy density for a particular transition. Stimulated emission is ignored. The above set of simultaneous equations is not linearly indepen-

dent, but it can be made so by eliminating one of the equations and substituting for it a normalizing equation:

$$\sum_{i=1}^{n} x_i = 1 .$$

As mentioned above, the molecular model includes a total of 206 energy levels leading to 206 equations in 206 unknowns. A matrix is set up and solved with a Gaussian elimination algorithm. Solution of this system of equations yields the relative population of the molecular energy levels. Once this quantity is known, the luminosity per molecule L/N (fluorescence efficiency) of a particular transition can be calculated from

$$(L/N)_{ij} = A_{ij} x_i h\nu_{ij} .$$

The band luminosity is just the summation of the above quantity over the transitions in a particular band. In this paper, the values of L/N will be given in both ergs s^{-1} per molecule and photons s^{-1} per molecule; the latter is often known as the "g factor."

b) *Transition Probabilities*

We employ the formulae for the Einstein A- and B-coefficients used by Schleicher and A'Hearn (1982):

$$A_{\rm line} = \frac{8\pi^2 e^2 \nu_{\rm line}^3 (2 - \delta_{0,\Lambda''}) f_{v'-v''} S_{\Sigma PJ}}{m_e c^3 \nu_{v'-v''} (2 - \delta_{0,\Lambda'+\Lambda''})(2J' + 1)} ,$$

and

$$B_{\rm line} = \frac{1}{8\pi h} \frac{c^3}{\nu_{\rm line}^3} \frac{(2J' + 1)}{(2J'' + 1)} A_{\rm line} ,$$

where $\nu_{v'-v''}$ is the frequency of the band origin (or zero line; see Herzberg 1950, p. 185), $f_{v'-v''}$ is the oscillator strength, and $S_{\Sigma PJ}$ is the Hönl-London factor for the transition. The Hönl-London factors for the Baldet-Johnson system are calculated using the normalization provided by Schleicher and A'Hearn (1982). The molecular parameters are taken from Rao (1950*a*, *b*) and Rao and Sarma (1953). The comet tail system, consisting of $^2\Pi$–$^2\Sigma$ transitions, employs the same equations as the $^2\Sigma$–$^2\Pi$ Baldet-Johnson system, except that each equation applies to a different term symbol (see Schadee 1964). The Hönl-London factors of the first negative system, $^2\Sigma^+$–$^2\Sigma^+$, are based on Schadee's (1964) equations with a renormalization. This follows from treating the Σ state rotational levels as two separate levels split by Hund's case b. A list of the normalized factors appears in Appendix A. Although this method gave rise to too many levels for the computer to solve in a reasonable amount of time, the procedure was followed for bookkeeping purposes. After all the necessary quantities were calculated, the coefficients for the transitions in and out of the doubled levels were combined to create the transition coefficients in and out of one level. It is assumed, as indicated by a preliminary calculation using separate levels, that the population in each component of the doubled levels is about the same, so that the appropriate Einstein A- and B-coefficients for the combined levels are just the averages of the values for the two components. This same procedure is followed for the Λ-doubled levels in the $A\ ^2\Pi_i$ state. This limits the size of the matrix yet retains the correctly normalized Hönl-London factors.

i) $A\ ^2\Pi$–$X\ ^2\Sigma^+$ *Transitions*

The wavenumbers for the vib-rotational transitions (which include all transitions up to rotational quantum number $N = 10$) are taken from Coster, Brons, and Bulthuis (1932), Schmid and Gerö (1933), and Rao (1950*b*). (The band numbering of Coster, Brons, and Bulthuis and of Schmid and Gerö was corrected as described by Rao.) The wavenumbers for the bands not included in the above references are calculated from the combination principle; the difference in wavenumbers between vib-rotational values from observed electronic transitions can yield the wavenumbers of unknown transitions. For example, to obtain rotational wavenumbers for the comet tail (0, 1) band, the appropriate vib-rotational wavenumbers from the Baldet-Johnson (0, 0) band are subtracted from the appropriate First Negative (0, 1) band wavenumbers. This procedure is followed to obtain any wavenumbers which are not tabulated. Wavenumbers for the (6, 0), (6, 1), and (6, 2) bands cannot be calculated in this fashion, and so they are calculated from constants and equations provided by Rao (1950*b*) and Herzberg (1950). The oscillator strengths for the comet tail system are obtained from Jain (1972). Although $f_{v'-v''}$ is not constant throughout a band, because of vibration-rotation interaction, the variation has been neglected since we are considering rotational levels only out to $N = 10$.

ii) $B\ ^2\Sigma^+$–$X\ ^2\Sigma^+$ *Transitions*

The transitions of the first negative system which occur in the UV (2000–2300 Å) have been studied extensively in the laboratory (for a list of authors see Krupenie 1966) and in comets (Feldman and Brune 1976). The wavenumbers for this system can be calculated to the required accuracy (0.01 Å) based on Rao's (1950*a*) constants and equations. Oscillator strengths for this system are obtained from Joshi, Sastri, and Parthasarati (1966).

iii) $B\ ^2\Sigma^+$–$A\ ^2\Pi$ *Transitions*

The Baldet-Johnson system (3600–4200 Å) has usually been neglected in the many studies of CO$^+$. It coincides with some of the comet tail transitions but is down at least two orders of magnitude in intensity. Detections of it in comets are relatively rare (Swings and Page 1950; Greenstein 1962). Consequently, data on this system are difficult to obtain. The calculations include the seven strongest Baldet-Johnson bands estimated from the Frank-Condon factors calculated by Nicholls (1962): the (0, 0), (0, 1), (0, 2), (1, 0), (1, 2), (2, 0), and (2, 1) bands. Wavenumbers for these bands come from Bulthuis (1934); as with other data from this period, the lower vibrational levels are misnumbered by 3. Various other constants are taken from Rao and Sarma (1953). To our knowledge, the oscillator strength for this system are not available, and an arbitrary value must be assigned to the oscillator strength so that the transition probabilities reflect laboratory observations by Lawrence (1965) and Judge and Lee (1972), which demonstrate that the transition probabilities are no more than 10% of the value of the comet tail system. This restriction on the Baldet-Johnson transition probabilities results in bands which are down in intensity by a factor of 10^3 from the stronger first negative and comet tail bands. This is consistent with their nondetection in most comets. The approach means that the predicted absolute intensities of the bands of the Baldet-Johnson system are very uncertain, but the relative intensities of the different bands of this system should still be reliable at the 20% level (see § IV).

Preliminary calculations indicated that the population in the A state was down by a factor of 10^8 from the population of the ground state. Thus, even though the Einstein B-coefficients for the $A\ ^2\Pi_i$–$B\ ^2\Sigma^+$ and $X\ ^2\Sigma^+$–$B\ ^2\Sigma^+$ transitions are of the same

TABLE 1

VALUES FOR THE EINSTEIN A BAND TRANSITION PROBABILITY

A. COMET TAIL SYSTEM

v'–v''	$A_{Band}(10^5\ s^{-1})$ $\Pi_{1/2}$	$\Pi_{3/2}$
0–0.....	0.40	0.39
0–1.....	1.01	0.99
0–2.....	1.01	0.99
1–0.....	1.35	1.31
1–1.....	1.84	1.79
1–2.....	0.60	0.58
2–0.....	2.34	2.29
2–1.....	1.29	1.26
2–2.....	0.44	0.43
3–0.....	2.76	2.71
3–1.....	0.28	0.27
3–2.....	0.69	0.68
4–0.....	2.53	2.44
4–1.....	0.03	0.03
4–2.....	1.26	1.20
5–0.....	2.22	1.90
5–1.....	0.61	0.52
5–2.....	0.97	0.83
6–0.....	1.41	1.21
6–1.....	1.28	1.09
6–2.....	0.21	0.18

B. FIRST NEGATIVE SYSTEM

v'–v''	$A_{Band}(10^7\ s^{-1})$
0–0.....	2.21
0–1.....	1.41
0–2.....	0.43
1–0.....	1.30
1–1.....	0.25
1–2.....	1.32
2–0.....	0.45
2–1.....	1.09
2–2.....	0.08

C. BALDET-JOHNSON SYSTEM

v'–v''	$A_{Band}(10^5\ s^{-1})$
0–0.....	6.01
0–1.....	3.79
0–2.....	1.59
1–0.....	7.31
1–2.....	1.93
2–0.....	2.93
2–1.....	6.89

order and the solar radiation density for the first negative system is down by a factor of 100, the pumping from the $A\ ^2\Pi_i$ to the $B\ ^2\Sigma^+$ state is smaller than the pumping from the $X\ ^2\Sigma^+$ to the $B\ ^2\Sigma^+$ state by a factor of 10^6. The pumping from the $A\ ^2\Pi_i$ state to the $B\ ^2\Sigma^+$ state is therefore ignored.

The Einstein A-coefficients for all electronic transitions are summarized in Table 1.

iv) *Pure Vibrational and Rotational Transitions*

Experimental values for A_{vib} and A_{rot} in the ground state are not available. *Ab initio* quantum mechanical calculations of A_{vib} (1–0) yield values of 8 and 20 s^{-1} (Rosmus and Werner 1982 and Chin and Person 1984 respectively). A canonical upper limit to the value of A_{vib} (1–0) for CO^+ may be determined from its parent molecule, CO, if it is assumed that A_{vib} scales as $\nu^3\mu^2$, where ν is the frequency of the desired transition and μ is the dipole moment. The quantity A_{vib} (1–0) for CO is 56 s^{-1} (Arpigny 1964*b*), μ for CO is 0.1 debyes (Kopelman and Klemperer 1962), and μ for CO^+ is 2.5 debyes (Certain and Woods 1973); with these values, A_{vib} for CO^+ is of order 10^4 s^{-1}. It is likely that A_{vib} and A_{rot} values for upper states are similar in magnitude to those of the ground state. In the upper electronic states, typical values of $A_{electronic}$ are 10^6–10^7 s^{-1}, so that the electronic transitions to and from the upper electronic states would proceed much faster than any purely rotational or vibrational transitions. Purely vibrational and purely rotational transitions are included only for the ground state. Arpigny (1964*b*) has also shown that within the levels of the $X\ ^2\Sigma^+$ state, A_{vib} values are sufficiently large that only pumping from the vibrational level $v'' = 0$ is important.

For selected cases calculations of the fluorescent equilibrium have been carried out using a variety of values for A_{vib} (1–0), A_{vib} (2–0), and A_{vib} (2–1). Since the individual values for these quantities are not well determined, the same value is used for all of them. For values of A_{vib} between 8 s^{-1} and 3.5×10^2 s^{-1}, the intensities of the first negative and comet tail features are virtually identical. Even for $A_{vib} = 3.5 \times 10^3$ s^{-1}, the band luminosities vary by no more than 4% from the $A_{vib} = 8$ s^{-1} band luminosities. The infrared emission, however, varies significantly with the value of A_{vib}.

The Einstein A-coefficients for the purely rotational transitions in the ground Σ state are obtained from formulae provided by Arpigny (1964*a*), using constants taken from Certain and Woods (1973) and from Rao (1950*a*). Microwave pumping of these transitions is ignored because the solar flux in that region of the spectrum is so low.

c) Solar Spectrum

For most of the required spectral range, a high-resolution, whole-disk solar atlas compiled by A'Hearn, Ohlmacher, and Schleicher (1983) expressly for the purpose of determining the fluorescence efficiency of cometary species is used. The atlas covers the spectral range from 2250 to 7000 Å with better than 1 km s^{-1} resolution. Several bands of the first negative system occur shortward of 2250 Å; those transitions include the (0, 0), (1, 0), (1, 1), (2, 0), (2, 1), and (2, 2) bands.

For this region of the spectrum, data from Broadfoot (1972) are used; unfortunately this atlas has a spectral resolution of only 1 Å. Because of this, the Swings effect for these bands cannot be included. Since these bands dominate the pumping into the $v' = 0$, 1, and 2 levels of the $B\ ^2\Sigma^+$ state, the calculations will not correctly predict the Swings effects for either the Baldet-Johnson system or the first negative system. Nevertheless, the Baldet-Johnson bands are only a minor contributor to the population of the $A\ ^2\Pi$ state, so the Swings effect of the comet tail system will be correctly predicted.

For the purpose of the calculations, the solar spectrum shortward of 2250 Å is represented by a series of straight lines connecting the midpoints of the bandpasses of Broadfoot's data. This leads to an effective flux of the pumping radiation which varies monotonically with Doppler shift. The resultant intensities of the first negative bands therefore vary systematically with Doppler shift by ~20%, suggesting that the results for these bands are reliable to about this accuracy. For the infrared region, which pumps the vibrational levels within the ground state, the solar spectral distribution given by Allen (1973) is interpolated. The Fraunhofer spectrum is smoother in this region so a large Swings effect is not expected.

IV. GENERAL THEORETICAL RESULTS

The relative populations of the 206 levels of the model for velocities ranging from -50 to $+350$ km s^{-1} in 5 km s^{-1} intervals at 1 AU from the Sun have been calculated. The population fractions for zero velocity are shown in Table 2; in Table 3 the fluorescence efficiencies of all bands in our model for a variety of velocities are presented. These values are obtained by adding the contributions of all lines in each band. As noted above, our results for the first negative and Baldet-Johnson systems ignore the Swings effect, but the ratios of first negative and comet tail bands should be correct to the accuracy indicated by the variations in the comet tail bands. Because values for the oscillator strengths of the Baldet-Johnson bands are not known, the absolute scale of the Baldet-Johnson system is not well known, but within that system the relative band intensities should be correct.

The Swings effects for the comet tail system are shown more clearly in a series of figures, and, as expected, the relative intensities change substantially as the heliocentric velocity changes. The fluorescence efficiencies for the (1, 0) and (2, 0) bands of the comet tail system are shown in Figure 2 in units of ergs s^{-1} per molecule and photons s^{-1} per molecule. These bands show 15%–20% variations in the fluorescence efficiency, while the (3, 0) band shows variations of up to 25%. The ratios of various bands normalized to the (2, 0) band are shown in Figure 3. Although velocity-dependent changes in fluorescence efficiency are evident in all these ratios, the most pronounced changes occur in the ratio of the $A\ ^2\Pi_{3/2}$ (red) and $A\ ^2\Pi_{1/2}$ (blue) components of the 3–0 band. Figure 4 shows these variations, which in some cases approach 50%. Even low-resolution spectra can separate the doublets (band heads are at 4017.8 and 3997.5 Å for the red and blue components, respectively, of the 3–0 band), allowing the ratios to be measured. Measurement of several of the above ratios at various positions in a comet's tail, even on low-dispersion spectra, can therefore be used to map the acceleration of CO$^+$ ions. Even in this case, the velocity-dependent Swings and Greenstein effects are not as marked as they are in the case of OH where the fluorescence efficiency of the 0–0 band varies by a factor of 7 (Schleicher and A'Hearn 1982). This is undoubtedly due to the fact that there is

TABLE 2

RELATIVE LEVEL POPULATIONS FOR $\dot{r}_H = 0$ km s^{-1}, $r_H = 1$ AU[a]

A.

	$X\ ^2\Sigma^+$			$B\ ^2\Sigma^+$		
N	$v = 0$	$v = 1$	$v = 2$	$v = 0$	$v = 1$	$v = 2$
0.....	1.17×10^{-1}	1.11×10^{-5}	3.25×10^{-6}	9.92×10^{-13}	6.22×10^{-13}	2.09×10^{-13}
1.....	1.38	0.81	1.88	11.78	7.43	2.66
2.....	1.19	1.22	3.40	14.59	9.18	3.25
3.....	1.29	1.28	3.45	12.90	8.12	2.89
4.....	1.15	1.16	3.09	12.68	7.82	2.84
5.....	1.04	1.02	2.72	10.91	6.64	2.38
6.....	0.89	0.86	2.32	9.20	5.63	2.03
7.....	0.66	0.71	1.86	7.82	4.72	1.73
8.....	0.56	0.60	1.49	5.73	3.55	1.25
9.....	0.42	0.43	1.14	4.26	2.66	0.97
10.....	0.25	0.25	0.72	4.45	2.87	1.03

B.

N	$v = 0$	$v = 1$	$v = 2$	$v = 3$	$v = 4$	$v = 5$	$v = 6$
				$A\ ^2\Pi_{3/2}(10^{-10})$			
1.....	9.85	16.38	19.57	20.04	5.22	5.04	2.97
2.....	8.71	14.42	16.28	15.29	5.25	3.54	2.19
3.....	7.07	13.89	10.18	9.04	4.47	3.67	2.31
4.....	5.05	11.85	9.91	11.87	4.47	3.36	2.22
5.....	5.46	11.13	6.30	6.75	4.50	3.24	2.07
6.....	5.14	9.25	6.06	6.66	3.18	2.64	1.30
7.....	3.28	7.01	5.66	7.09	3.36	1.54	1.27
8.....	2.97	5.60	5.80	2.82	1.99	1.15	0.74
9.....	2.70	3.67	3.76	3.90	2.21	0.77	0.58
10.....	2.01	3.65	2.85	3.82	1.80	0.61	0.56
				$A\ ^2\Pi_{1/2}(10^{-10})$			
1.....	5.23	9.71	9.72	7.72	5.21	1.44	0.87
2.....	6.10	9.74	11.36	11.23	6.09	2.03	1.42
3.....	6.04	11.21	10.72	10.86	6.50	2.05	1.53
4.....	6.10	11.96	10.01	10.27	6.58	1.85	1.24
5.....	5.44	10.87	10.14	11.01	6.12	2.51	1.24
6.....	5.92	6.30	9.26	7.88	4.24	1.37	0.95
7.....	4.32	7.45	5.99	4.67	3.96	1.32	1.02
8.....	3.83	6.05	5.66	4.38	2.38	1.07	0.71
9.....	2.34	4.16	4.03	4.77	2.17	0.39	0.63
10.....	2.46	3.50	2.76	2.11	2.01	0.53	0.13

[a] H = heliocentric.

TABLE 3

BAND LUMINOSITIES AT $r_H = 1$ AU

A. COMET TAIL SYSTEM[a] ($A\ ^2\Pi_i$–$X\ ^2\Sigma^+$) L/N[b]

	BAND HEAD		$\dot{r}_H$ (km s^{-1})							
v'–v''	$\Pi_{1/2}$	$\Pi_{3/2}$	−50	0	50	100	150	200	250	300
0–0	4880	4910	0.18	0.16	0.18	0.17	0.17	0.17	0.18	0.18
0–1	5461	5500	0.40	0.36	0.40	0.38	0.37	0.38	0.41	0.40
0–2	6189	6239	0.35	0.32	0.36	0.34	0.33	0.33	0.36	0.35
1–0	4540	4566	1.00	1.03	0.97	1.00	0.97	1.01	1.04	1.00
1–1	5039	5073	1.22	1.27	1.19	1.23	1.19	1.24	1.27	1.22
1–2	5653	5694	0.35	0.36	0.34	0.35	0.34	0.36	0.36	0.35
2–0	4249	4272	1.86	1.79	1.56	1.69	1.59	1.56	1.74	1.62
2–1	4684	4712	0.93	0.89	0.78	0.85	0.79	0.78	0.87	0.81
2–2	5209	5244	0.28	0.27	0.24	0.26	0.24	0.24	0.26	0.25
3–0	3998	4018	2.17	2.20	2.04	2.24	2.04	2.14	2.10	2.14
3–1	4379	4403	0.20	0.20	0.19	0.21	0.19	0.20	0.19	0.20
3–2	4837	4866	0.45	0.45	0.42	0.46	0.42	0.44	0.43	0.44
4–0	3778	3796	1.07	1.07	1.10	1.01	0.99	0.94	1.04	1.03
4–1	4117	4139	0.01	0.01	0.01	0.01	0.01	0.01	0.01	0.01
4–2	4518	4544	0.44	0.44	0.45	0.42	0.41	0.39	0.43	0.43
5–0	3584	3601	0.39	0.42	0.44	0.41	0.44	0.40	0.44	0.40
5–1	3889	3908	0.10	0.11	0.11	0.10	0.11	0.10	0.11	0.10
5–2	4244	4268	0.14	0.16	0.16	0.15	0.16	0.15	0.16	0.15
6–0	3413	3428	0.18	0.18	0.16	0.19	0.17	0.19	0.21	0.20
6–1	3688	3705	0.15	0.15	0.14	0.16	0.14	0.16	0.17	0.17
6–2	4002	4020	0.02	0.02	0.02	0.02	0.02	0.02	0.03	0.02

B. FIRST NEGATIVE SYSTEM ($B\ ^2\Sigma^+$–$X\ ^2\Sigma^+$)[a] L/N[c]

v'–v''	Band Head	L/N
0–0	2190	1.97
0–1	2300	1.20
0–2	2419	0.35
1–0	2112	0.71
1–1	2214	0.13
1–2	2325	0.66
2–0	2042	0.10
2–1	2138	0.23
2–2	2240	0.02

C. BALDET-JOHNSON SYSTEM ($B\ ^2\Sigma^+$–$A\ ^2\Pi_i$)[a] L/N[c]

	BAND HEADS		
v'–v''	$\Pi_{1/2}$	$\Pi_{3/2}$	L/N
0–0	3975	3955	0.30
0–1	4233	4210	0.17
0–2	4521	4495	0.07
1–0	3726	3709	0.23
1–1	3950	3930	<0.01
1–2	4203	4180	0.06
2–0	3513	3498	0.04
2–1	3713	3695	0.08
2–2	3920	3910	<0.01

[a] Band heads are in units of Å in vacuo; values for Baldet-Johnson system are approximate.
[b] In 10^{-14} ergs s^{-1}.
[c] In 10^{-15} ergs s^{-1}.

significant population of many more rotational levels for CO^+ than for OH. As discussed above, the Swings effects for the first negative and Baldet-Johnson systems were not calculated.

Table 4 shows the calculated results for two arbitrarily chosen velocities compared with observations made by Arpigny (1964*b*) on comet Humason 1962 VIII. Also listed are the results of the fluorescence calculations by Krishna Swamy (1979), who neglected velocity effects. All the bands are normalized to the (2, 0) band for the comet tail system and to the (0, 0) band for the first negative system. It must be noted, however, that Arpigny's observations were made when the comet was at 2.6 AU, while the tabulated results are calculated for 1 AU. No attempt has been made to estimate the appropriate radial velocity for these observations and so the velocities are chosen arbitrarily, except to require that they be greater than the radial velocity of the cometary nucleus. Also included are the observations of Feldman and Brune (1976) on comet West 1976 VI for the B–X transition of CO^+. The estimated areas of the profiles normalized to the (0, 0) band are taken from estimates by Krishna Swamy (1979). As in the previous case, the results are for 1.0 AU, while in this case, the spectra were obtained when comet West was at 0.39 AU.

An examination of Table 3 shows that the tabulated results agree with the observations somewhat better than do those of Krishna Swamy. The observations of the first negative system include the 1–3 and 2–4 bands, which were not included in the calculations. Their contribution (in photon units) can be estimated as $A_{13}/A_{10} \times (L/N)_{10}$ and $A_{24}/A_{20} \times (L/N)_{20}$, respectively, leading to the value given in the table for the sum of the three blended features.

The calculations also predict the Swings effects for individual vib-rotational lines in each of the comet tail bands. Figure 5*a* shows how the fluorescence efficiencies of the individual lines of the $Q_1 + {}^PQ_{12}$ branches (which virtually coincide) of the 3–0 comet tail band differ for two different heliocentric velocities, $v = 95$ km s^{-1} and $v = 130$ km s^{-1}. Figure 5*b* shows the corresponding results for the $Q_2 + {}^RQ_{21}$ branches. It is clear from these figures that observations of the rotational

TABLE 4

A.

RELATIVE INTENSITIES OF A–X BANDS OF CO^+

BAND	KRISHNA SWAMY (1979)	THIS WORK (r_H = 1 AU) $\dot{r}_H$ = 125 km s^{-1}	THIS WORK (r_H = 1 AU) $\dot{r}_H$ = 170 km s^{-1}	OBSERVATIONS[a] (r_H = 2.6 AU)
(0, 0).....	0.07	0.11	0.11	0.12
(1, 0).....	0.53	0.64	0.63	0.60
(2, 0).....	1.00	1.00	1.00	1.00
(2, 1).....	0.39	0.50	0.50	0.43
(3, 0).....	1.01	1.21	1.20	1.16
(3, 2).....	0.19	0.25	0.27	0.25
(4, 0).....	0.58	0.60	0.67	0.64
(4, 2).....	0.17	0.25	0.28	0.26
(5, 0).....	0.35	0.29	0.28	0.40
(6, 1).....	0.12	0.09	0.11	0.16

B.

RELATIVE INTENSITIES OF B–X BANDS OF CO^+

BAND	KRISHNA SWAMY (1979)	THIS WORK (r_H = 1 AU)	OBSERVATIONS[b] (r_H = 0.39 AU)
(0, 0).....	1.00	1.00	1.00
(1, 0).....	0.27	0.34	0.35
(0, 1), (1, 2).....	0.71	0.92	0.92
(0, 2), (1, 3), (2, 4).....	0.25	0.52[c]	0.42

[a] From Arpigny 1964*b*; normalized to (2, 0) band.

[b] Estimates by Krishna Swamy 1979 of spectrum by Feldman and Brune 1976; normalized to (0, 0) band.

[c] Our calculations include only the (0, 2) band. We estimate the contribution from the (1, 3) and (2, 4) bands as described in the text. The contribution from these two bands is 0.35 as normalized to (0, 0) band.

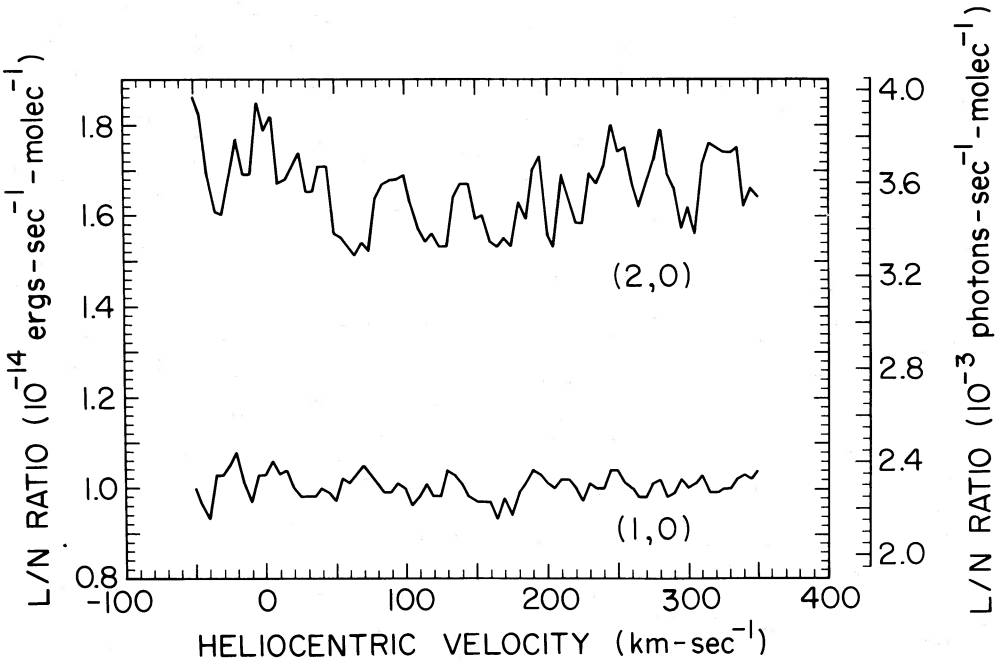

FIG. 2.—Fluorescence efficiencies of the (1, 0) and (2, 0) comet tail bands at r_H = 1 AU, as a function of heliocentric radial velocity. The ordinate scales are given both in energy units and in photon units, the latter units being more common when the quantity is called the "g-factor."

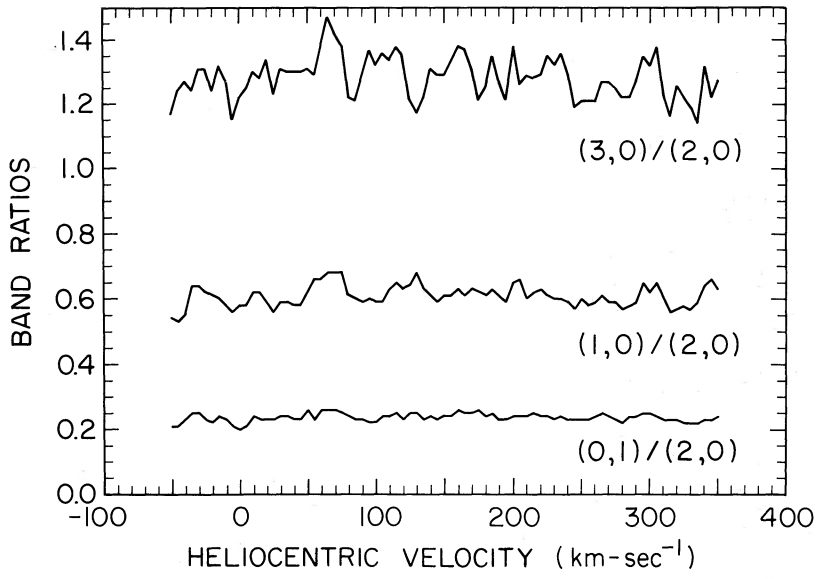

FIG. 3a

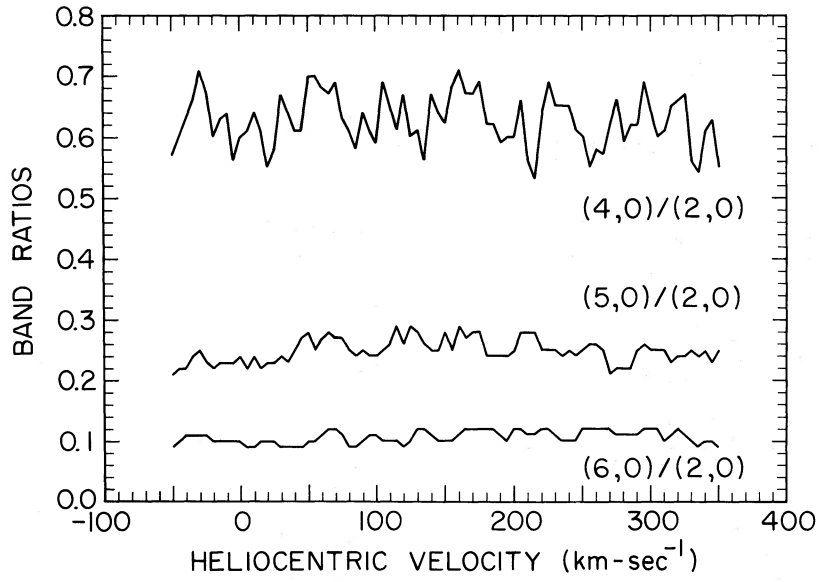

FIG. 3b

FIG. 3.—(*a*) Fluorescence efficiency of the (0, 1), (1, 0), and (3, 0) comet tail bands at $r_H = 1$ AU normalized to the (2, 0) band as a function of heliocentric velocity. Intensity units; for photon units multiply by $\lambda_x/\lambda_{(2-0)}$. (*b*) Fluorescence efficiency of the (4, 0), (5, 0), and (6, 0) comet tail bands normalized to the (2, 0) band as a function of heliocentric velocity. Units as in (*a*).

structure of this band could be used to map the velocity, and thus the acceleration, of the CO^+ ions in comets. This point will be addressed explicitly in a subsequent paper.

V. CONCLUSIONS

The spectrum of CO^+ as produced by the Swings fluorescence mechanism in the radiation field of the Sun at 1 AU was calculated. The calculations include pumping in the *B–X*, *A–X*, and *X–X* (vibrational transitions only) systems and emission in the *B–A*, *B–X*, *A–X*, and *X–X* (vibrational and rotational transitions) systems. Stimulated emission and rotational and vibrational transitions within the $A\ ^2\Pi_i$ and $B\ ^2\Sigma^+$ states and the detailed hyperfine structure are ignored. The model includes 10 rotational levels in each vibrational level and the heretofore ignored Baldet-Johnson transitions along with a detailed solar atlas. Our results compare favorably with the few quantitative CO^+ observations which are available. The Swings fluorescence mechanism can therefore adequately account for all extant observations of the comet tail and first negative systems. In addition, the changes in fluorescence efficiencies and band ratios as a function of heliocentric velocity for some of the transitions are given. These calculations, in conjunction with low-resolution spectroscopy of integrated band luminosities or with high-resolution spectroscopy of individual rotational lines along cometary ion tails, may allow the mapping of the velocity structure in cometary tails. This result would determine whether material executes bulk motion down the cometary tail or whether this motion is a manifestation of a hydromagnetic wave phenomena.

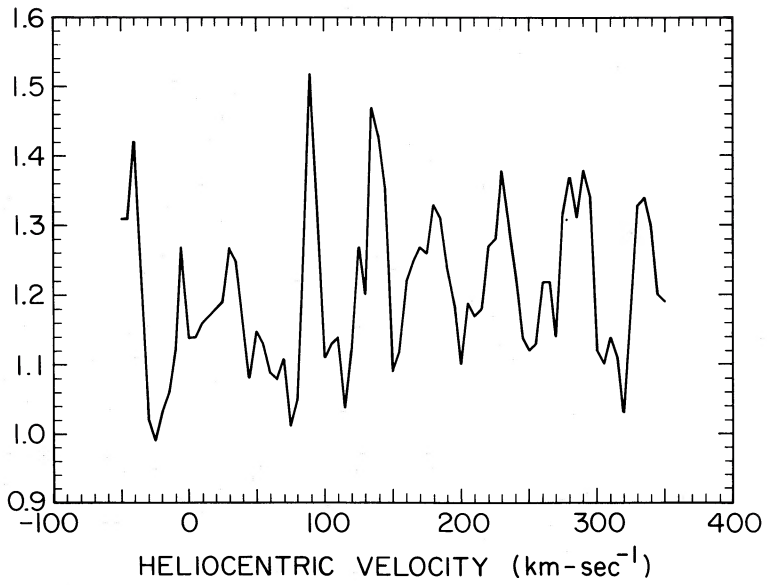

FIG. 4.—Ratio of the fluorescence efficiency of the red ($A\ ^2\Pi_{3/2}$) to blue ($A\ ^2\Pi_{1/2}$) components of the (3, 0) comet tail band as a function of heliocentric velocity

We thank J. Ohlmacher, A. Magnani, and D. Klinglesmith for programming assistance and D. Schleicher, W. Benesch, J. Bonnell, and C. Arpigny for many fruitful discussions. Computer time was provided by the University of Maryland Computer Science Center. We acknowledge partial support from NASA grant NSG 7322.

APPENDIX A

The Hönl-London factors for $^2\Sigma^+$–$^2\Sigma^+$ transitions are given by Schadee (1964). We renormalize these equations so that they conform to

$$\sum_{p'p''} \sum_{\Sigma'\Sigma''} \sum_{N'} S_{\Sigma Np} = (2 - \delta_{0,\,\Lambda'+\Lambda''})(2S + 1)(2N' + 1)\,,$$

where S (no superscript) is the spin, Σ is the electronic substate due to spin multiplicity, N is the rotational quantum number apart from spin, Λ is the component of the electronic angular momentum along the internuclear axis, p is the parity, and single and double primes indicate upper and lower levels, respectively. This normalization is appropriate to our original model before the levels were combined and, for the $^2\Sigma^+$–$^2\Sigma^+$ transition, is the same as the normalization used by Schleicher and A'Hearn (1982). The Hönl-London factors we employ are

$$P_1: \quad \frac{2N''(N'' + 1)}{2N'' + 1}\,,$$

$$R_1: \quad \frac{2(N'' + 1)(N'' + 2)}{2N'' + 3}\,,$$

$$^RQ_{21}: \quad \frac{2(N'' + 1)}{(2N'' + 1)(2N'' + 3)}\,,$$

$$^PQ_{12}: \quad \frac{2N''}{(2N'' - 1)(2N'' + 1)}\,,$$

$$P_2: \quad \frac{2N''(N'' - 1)}{2N'' - 1}\,,$$

$$R_2: \quad \frac{2N''(N'' + 1)}{2N'' + 1}\,.$$

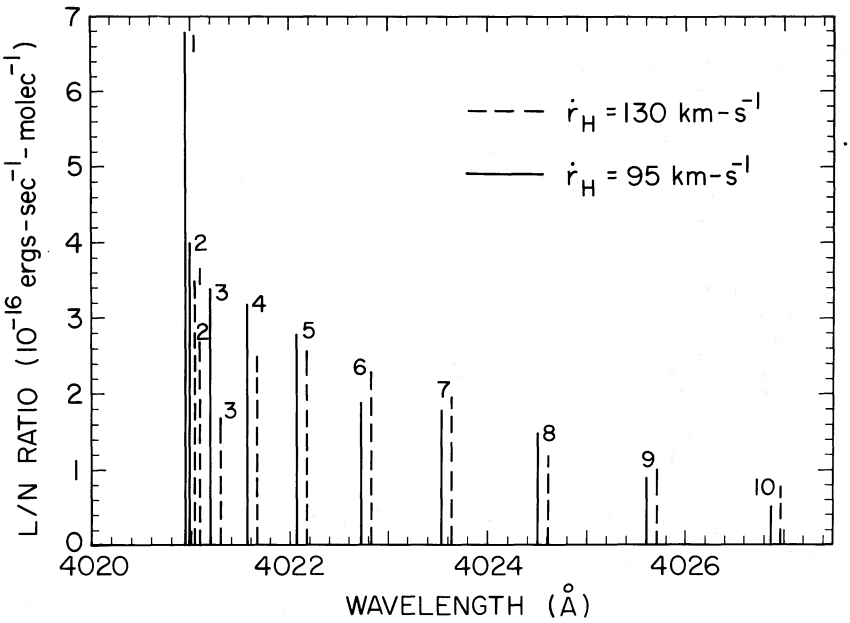

FIG. 5a

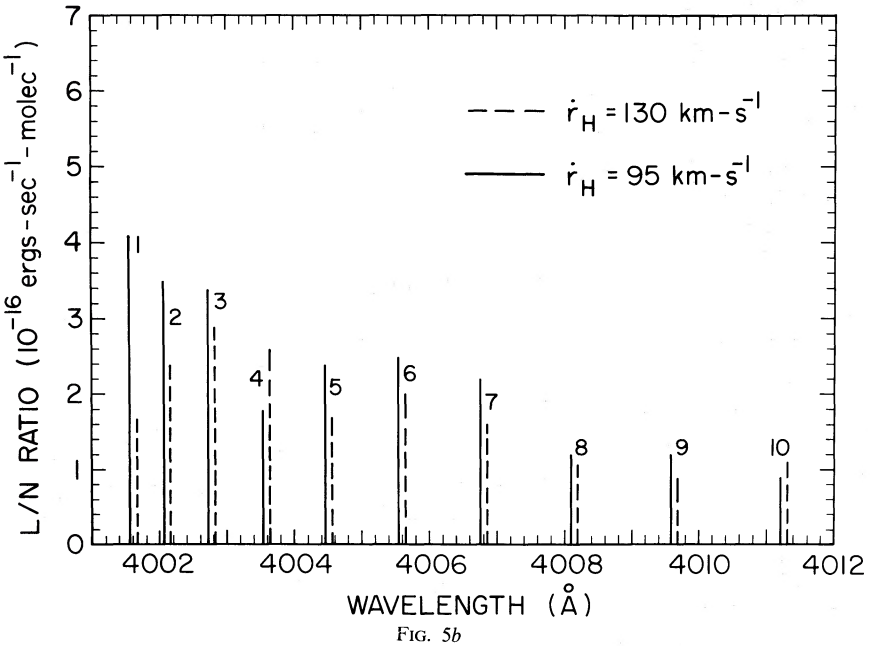

FIG. 5b

FIG. 5.—(*a*) Fluorescence efficiencies of the $Q_1 + {}^PQ_{12}$ rotational lines of the (3, 0) comet tail band for two heliocentric velocities: $v = 95$ km s^{-1} and $v = 130$ km s^{-1}. The rotational lines for $v = 130$ km s^{-1} are shifted 0.1 Å to the right for more clarity. The lines are labeled with the value of $N'' = J'' + \frac{1}{2}$. (*b*) Same as (*a*), but for $Q_2 + {}^RQ_{21}$ rotational lines labeled with the value of $N'' = J'' - \frac{1}{2}$.

REFERENCES

A'Hearn, M. F., Ohlmacher, J. T., and Schleicher, D. G. 1983, University of Maryland Tech. Rept., TR AP83-044.
Allen, C. W. 1973, *Astrophysical Quantities* (3d ed.; London: Athlone).
Arpigny, C. 1964*a*, *Ann. d'Ap.*, **27**, 393.
———. 1964*b*, *Ann. d'Ap.*, **27**, 406.
———. 1976, in *The Study of Comets*, ed. B. Donn, M. Mumma, W. Jackson, M. A'Hearn, and R. Harrington (Washington: NASA SP-393), p. 797.
Brandt, J. C., and Mendis, D. A. 1979, in *Solar System Plasma Physics*, Vol. **2**, ed. C. F. Kennel, L. J. Lanzerotti, and E. N. Parker (Amsterdam: North Holland), p. 253.
Broadfoot, A. L. 1972, *Ap. J.*, **173**, 681.
Bulthuis, H. 1934, *Physica*, **1**, 873.
Certain, P. R., and Woods, R. C. 1973, *J. Chem. Phys.*, **58**, 5837.
Chin, S., and Person, W. B. 1984, *J. Phys. Chem.*, **88**, 553.
Coster, D., Brons, H. H., and Bulthuis, H. 1932, *Zs. Phys.*, **79**, 787.
Crovisier, J. 1985, *A.J.*, **90**, 670.
Delsemme, A. H. 1982, in *Comets*, ed. L. L. Wilkening (Tucson: University of Arizona Press), p. 85.
Feldman, P. D., and Brune, W. H. 1976, *Ap. J. (Letters)*, **209**, L45.
Greenstein, J. L. 1958, *Ap. J.*, **128**, 106.
———. 1962, *Ap. J.*, **136**, 668.
Herzberg, G. H. 1950, *Molecular Spectra and Molecular Structure. I. Spectra of Diatomic Molecules* (New York: Van Nostrand).
Jain, D. C. 1972, *J. Phys. B, Atomic Molec. Phys.*, **5**, 194.
Jarmain, W. R., Fraser, P. A., and Nicholls, R. W. 1955, *Ap. J.*, **122**, 55.
Joshi, K. C., Sastri, V. D. P., and Parthasarati, S. 1966, *J. Quant. Spectrosc. Rad. Transf.*, **6**, 215.
Judge, D. L., and Lee, L. C. 1972, *J. Chem. Phys.*, **57**, 455.

Kopelman, R., and Klemperer, W. 1962, *J. Chem. Phys.*, **36**, 1693.
Krishna Swamy, K. S. 1979, *Ap. J.*, **227**, 1082.
Krupenie, P. H. 1966, NSRDS-NBS-5, No. 5.
Lawrence, G. M. 1965, *J. Quant. Spectrosc. Rad. Transf.*, **5**, 359.
Miller, F. D. 1980, *A.J.*, **85**, 468.
Nicholls, R. W. 1962, *Canadian J. Phys.*, **40**, 1772.
Rao, K. N. 1950*a*, *Ap. J.*, **111**, 50.
———. 1950*b*, *Ap. J.*, **111**, 306.
Rao, K. N., and Sarma, K. S. 1953, *Mém. Soc. Roy. Sci. Liège*, **13**, 181.
Rosmus, P., and Werner, M. J. 1982, *J. Molec. Phys.*, **47**, 661.
Schadee, A. 1964, *Bull. Astr. Inst. Netherlands*, **17**, 311.
Schleicher, D. G., and A'Hearn, M. F. 1982, *Ap. J.*, **258**, 864.
Schmid, R., and Gerö, L. 1933, *Zs. Phys.*, **86**, 297.
Swings, P. 1941, *Lick Obs. Bull.*, Vol. **19**, No. 508, p. 131.
Swings, P., and Page, T. L. 1950, *Ap. J.*, **111**, 530.
Wyckoff, S., and Wehinger, P. 1976, *Ap. J.*, **204**, 604.

MICHAEL F. A'HEARN and LORIS MAGNANI: Astronomy Program, University of Maryland, College Park, MD 20742